Society For Biomaterials

Short and long gap peripheral nerve repair with magnesium metal filaments

Tracy M. Hopkins,[1] Kevin J. Little,[2] John J. Vennemeyer,[1] Jefferson L. Triozzi,[3] Michael K. Turgeon,[3] Alexander M. Heilman,[3] D. Minteer,[4] K. Marra,[5] David B. Hom,[6] Sarah K. Pixley[1]*

[1]Department of Pharmacology and Systems Physiology, University of Cincinnati College of Medicine, 231 Albert Sabin Way, Cincinnati, Ohio 45267
[2]Division of Pediatric Orthopaedics, Cincinnati Children's Hospital Medical Center, 3333 Burnet Ave, Cincinnati, Ohio 45229
[3]Student Affairs, University of Cincinnati College of Medicine, 231 Albert Sabin Way, Cincinnati, Ohio 45267
[4]Department of Plastic Surgery, University of Pittsburgh, 3380 Boulevard of the Allies, Suite 138, Pittsburgh, Pennsylvania 15213
[5]Departments of Plastic Surgery and Bioengineering, 1655E BST, University of Pittsburgh, 200 Lothrop St., Pittsburgh, Pennsylvania 15261
[6]Division of Facial Plastic & Reconstructive Surgery, Department of Otolaryngology-Head and Neck Surgery, University of Cincinnati College of Medicine, 231 Albert Sabin Way, Cincinnati, Ohio 45267

Received 14 May 2017; revised 28 June 2017; accepted 1 August 2017
Published online 24 August 2017 in Wiley Online Library (wileyonlinelibrary.com). DOI: 10.1002/jbm.a.36176

Abstract: A current clinical challenge is to replace autografts for repair of injury gaps in peripheral nerves, which can occur due to trauma or surgical interruption. Biodegradable metallic magnesium filaments, placed inside hollow nerve conduits, could support nerve repair by providing contact guidance support for axonal regeneration. This was tested by repairing sciatic nerves of adult rats with single magnesium filaments placed inside poly(caprolactone) nerve conduits. Controls were empty conduits, conduits containing titanium filaments and/or isografts from donor rats. With a nerve gap of 6 mm and 6 weeks post-repair, magnesium filaments had partially resorbed. Regenerating cells had attached to the filaments and axons were observed in distal stumps in all animals. Axon parameters were improved with magnesium compared to conduits alone or conduits with single titanium filaments. With a longer gap of 15 mm and 16 weeks post-repair, functional parameters were improved with isografts, but not with magnesium filaments or empty conduits. Magnesium filaments were completely resorbed and no evidence of scarring was seen. While axon outgrowth was not improved with the longer gap, histological measures of the tissues were improved with magnesium compared to empty conduits. Therefore, the use of magnesium filaments is promising because they are biocompatible and improve aspects of nerve regeneration. © 2017 Wiley Periodicals, Inc. J Biomed Mater Res Part A: 105A: 3148–3158, 2017.

Key Words: peripheral nerve repair, magnesium metal, biodegradable metal, biocompatibility, sciatic nerve

How to cite this article: Hopkins TM, Little KJ, Vennemeyer JJ, Triozzi JL, Turgeon MK, Heilman AM, Minteer D, Marra K, Hom DB, Pixley SK. 2017. Short and long gap peripheral nerve repair with magnesium metal filaments. J Biomed Mater Res Part A 2017:105A:3148–3158.

INTRODUCTION

When peripheral nerve injury results in a gap that cannot be closed without tension, the current gold standard of clinical care for nerve repair is to replace the gap with an autograft.[1] Because the use of an autograft requires a concurrent surgery at a separate site, compromises an intact donor nerve and still does not result in a success rate of 100%, other options are being researched.[2–4] Hollow biomaterial nerve conduits (guides), made of either natural or synthetic materials, are in clinical use and provide functional recovery for relatively short nerve gaps of around 25 mm.[1,5] For gaps longer than this critical length limit, conduits alone do not result in repair. One hypothesis suggests that hollow conduits require additional internal structures to duplicate the extracellular matrix components and fibrin clot materials that provide contact guidance and physically support fibroblasts and Schwann cells as they cross gaps.[6,7] Schwann cells then form columns of cells (bands of Büngner) that support axonal regeneration.[3,4] Several linearized materials have been tested for providing

*Portions of this work have appeared previously in abstract and poster format
Correspondence to: Sarah Pixley; e-mail: Sarah.pixley@uc.edu
Contract grant sponsor: NSF ERC for Revolutionizing Metallic Biomaterials; contract grant numbers: EEC-0812348, NCAT 260116 C
Contract grant sponsors: American Association of Hand Surgeons, Annual Research Grant; University of Cincinnati Department of Otolaryngology-Head and Neck Surgery

internal support, from polyspun fiber sheets to silk fibers,[8,9] with or without adding living cells.[1,4] Processed, acellular nerve grafts, which contain extracellular matrix components, also show promise.[10] We propose that microfilaments of the biodegradable metal magnesium (Mg) might also provide linear support. Mg has benefits over many of the other biomaterials, including a more rapid rate of degradation and technical simplicity.

Mg metal is being explored as a biodegradable medical implant material because it provides significant advantages over inert metals and biodegradable plastics.[11,12] While it is not currently FDA approved for medical implant use, a screw for fixation of the big toe received a European CE mark in 2013 and is being used clinically in Europe.[13] Mg cardiovascular stents are also in clinical trials in Europe.[11,14] Difficulties that are challenging for Mg in orthopaedic uses include that both pure and current alloyed forms of Mg are not strong enough for weight-bearing bone repair, most forms of Mg degrade too fast to provide sufficient physical support throughout the healing process and rapid degradation of Mg *in vivo* oxidizes water, releasing hydrogen gas bubbles and increasing pH (via release of OH^- ions).[11,14] Thus, research has focused on improving Mg strength and controlling resorption rate by using different alloys, surface treatments and coatings.[14]

We proposed using Mg metal filaments inside nerve conduits for nerve repair because the metal would easily provide the strength to physically support cells across the gap and all animal studies to date suggest that Mg degrades without untoward soft tissue reaction. In addition, Mg degradation releases soluble Mg^{2+} and hydrogen gas (H_2), both of which have interesting neuroprotective and anti-oxidant properties[15,16] and thus could influence nerve regrowth. In a previous study, we showed that Mg metal presence did not damage regenerating nerve tissues.[17] We have expanded these studies herein, continuing to examine biocompatibility and efficacy, examining two gap sizes in rats and with both short and long time-periods of recovery.

METHODS

Filament preparation

Mg filaments (99.9% pure Mg wire, Goodfellow, Coraopolis, PA) and control titanium (Ti) filaments (Goodfellow) were 0.25 mm diameter. Mg filaments, delivered wrapped on a spool, were straightened to overcome the shape memory and prevent distortion of the nerve guides. This was done by rolling the wire gently between two cleaned glass plates before being cut, cleaned (sonicated in 100% ethanol, 10 min), dried and sterilized (UV exposure, 20 min per side) prior to implantation.

PCL conduits

PCL conduits were prepared as previously described.[18,19] This involved, in brief, dipping glass mandrels (1.5 mm diameter) into a liquid slurry of PCL (average MW ~65,000, average Mn ~42,500, pellets), ethyl acetate and NaCl crystals (ground and sieved to sizes that would create pore diameters of 10–38 μm), resulting in 80% porosity percentage of the guides after air drying. Wall thickness was ~0.6 mm, adjusted by repeating dipping. Reagents (analytical grade or better) were from Sigma–Aldrich, St. Louis, MO. Conduits were cut to size and sterilized using ethanol.

Animals and surgery

All animal treatment protocols were approved by the University of Cincinnati Institutional Animal Care and Use Committee (IACUC), were in accordance with the Guide for the Care and Use of Laboratory Animals, as adopted by the NIH, and were done in AAALAC approved facilities. A total of 47 adult female Lewis rats (Harlan, Indianapolis, IN) were used, weighing 180 to 200 g at surgery. Animals were anesthetized (isoflurane gas) and the right sciatic nerve was exposed, transected five mm proximal to the sciatic/peroneal bifurcation and allowed to retract for 30 seconds, as described previously.[17,19] In one experimental series, a short nerve gap of 6 mm (less than the supposed critical gap length in rats) was created by inserting both nerve stumps into an 8 mm long PCL nerve conduit, overlapping nerve stumps by one mm and suturing conduits to the nerve epineurium (8–0 polypropylene, Ethicon Endo Surgery, NJ). In two groups, a single Mg or Ti filament (10 mm long, 0.25 mm diameter) was inserted inside conduits, extending two mm into both stumps. In a second experimental series, a "long" gap of 15 mm was made and filled with a 17 mm long PCL conduit, overlapping the nerve stumps by 1 mm. In the experimental group, a 20 mm Mg filament was placed inside each conduit, extending 2.5 mm into each nerve stump. Conduit lumens were filled via syringe with sterile 0.9% saline and overlying muscles and skin were closed (4–0 Vicryl sutures, Ethicon Endo Surgery, NJ). Lidocaine HCl gel (Akorn, IL) was applied to the wound and injured legs and feet were sprayed after surgery and then approximately weekly with Bitter Apple Spray (Petsmart, Cincinnati, OH) to prevent autophagy. While toenail chewing was seen, rarely and randomly across all groups, no other signs of autophagy or animal discomfort were observed.

The experimental groups ($n = 7$ rats/group, 21 rats) for the short gap were: repairs with (1) Empty conduits (Em), (2) conduits plus a single Ti filament, and (3) conduits plus a Mg filament. The Ti group tests the hypothesis that metal filaments of any kind could provide a physical support for cells to cross the gap. For the long gap, the groups were (1) Empty conduits (Em, $n = 7$), (2) conduits plus a Mg filament (Mg, $n = 7$), and (3) isografts (Iso, $n = 8$) (22 animals plus 4 donor rats). Nerve grafts, from donor animals of the same sex, weight, and strain as experimentals, were 15 mm long after allowing for nerve retraction. They were reversed at placement and sutured to the epineurium of hosts.

Functional assessments

The first functional assessment in living animals was to measure the diameter of both hind legs in living animals at the level of the belly of the triceps surae (calf) muscle, to monitor muscle atrophy and subsequent recovery. Second, to monitor sensory function, a skin flap or toes were

pinched with blunt, fine-tipped (2 mm) forceps, monitoring reactions (retraction or vocalization). A scale was assigned according to pinch location (modified from Ref. 20). Locations were: a skin flap at the back of the ankle (1 if positive), a skin flap on the lateral side of the ankle (2 if positive), a skin flap on the lateral side of the anterior foot at the base of the lateral toe (3 if positive) and a pinch between the joints of the lateral toe (toe #5, 4 if positive), Responses of toes # 3 and 4 were highly variable and omitted from analysis. Care was taken to avoid moving the toe, foot or a larger section of skin, responses were compared to comparable pinches on the uninjured foot and areas were tested at least twice. In experimental feet, there were no reactions (0) at 1 week post-surgery. Finally, as a measure of motor recovery, reflex extension of the lateral toe was scored (modified from Ref. 20). With the rat raised by its tail, standing on its front feet, a score of 0 indicated an immobile toe held straight and tightly against the foot. A score of 1 indicated slight motion, either curling (contraction) or lateral movement (sideways abduction). A score of 2 indicated definite movement (more extensive curling, lateral abduction or a combination of curling and lateral abduction) and a 3 indicated full lateral extension and some dorsal extension (uncurling). Normal toe motion was a 4, with full lateral and dorsal extension.

Animal sacrifice and tissue processing

Animals with short gaps were sacrificed at 6 weeks post-surgery and animals with long gaps at 16 weeks post-surgery. Prior to sacrifice, animal weights and uninjured calf sizes did not differ significantly between animals or groups. At sacrifice, conduits plus ~2–5 mm of both nerve stumps and contralateral nerves were removed, attached to a solid support and fixed [4% paraformaldehyde in phosphate buffered saline (PBS)]. All conduits appeared similar by visual examination. Calf muscles (including both heads of the gastrocnemius and plantaris, but not soleus) from both legs were removed and immediately weighed. With short gap animals, tissues were imaged via micro computed tomography (micro-CT) at 1–3 h after removal to determine Mg degradation status. The imaging was performed immediately to avoid further metal degradation during processing. The tissues were then returned to fixative for 48 h, after which tissues for histology were paraffin embedded (standard methods), while those prepared for micro-CT of soft tissues were post-fixed in osmium tetroxide (1%, 48 h), rinsed and embedded in Epon (Sigma–Aldrich).

Micro-CT imaging

To assess Mg filament degradation at 6 weeks, conduits containing Mg were imaged via micro-CT on the day of sacrifice. Ti filaments were not imaged (no changes expected), nor were tissues from the long-term experiment, where Mg degradation was estimated to be complete (confirmed by histology). For long-gap tissues, the distal halves of the conduits were fixed with osmium to impart soft tissue density and imaged via micro-CT. Imaging was done in a Siemens Inveon Multimodality System (San Diego, CA) in the University of Cincinnati Vontz Core Imaging Laboratory. Samples were scanned at half-degree increments with 384 steps (step and shoot) for 192°. Images were acquired with high magnification and a pixel matrix binning of two, resulting in an effective voxel size of 17.27 μm, using 80 kVp voltage and 300 μA current, with the exposure time at 2100 ms with 25 ms settle time. All tissues were kept moist in PBS during the ~1 h scan, with up to 8 conduits placed in a Styrofoam boat, as shown previously.[17] Image analysis and preparation of figures was done with either the Inveon software or ImageJ (NIH, exporting image stacks as DICOM files), using either 3 D reconstructions or single frames. Using the Inveon software, tissues with similar Hounsfield Unit (HU) radiodensities were selected and either measured or cut out into a new file and rendered into 3 D images.

Tissue sectioning and staining

Paraffin embedded tissue sections (10-μm thick) were stained with hematoxylin & eosin (H&E) or Masson's trichrome (kit from Newcorner Supply, Middleton, WI) and coverslipped (Permount). Sections that were immunostained (standard methods[17]) used incubations of 1 h for blocking buffer (10% serum and 0.1% Triton X100 in PBS), 18 h for primary antibodies and 2 h for secondaries (room temperature, PBS rinses) and were coverslipped with Fluoromount (Fisher Scientific, Pittsburgh, PA). Primary antibodies labeled (1) axons (rabbit antibody to 200 MW neurofilament protein (NF), 1:500 dilution, Sigma–Aldrich), (2) Schwann cells (rabbit antibody to the protein S100, 1:500, Dako, Carpenterio, CA), (3) macrophages (mouse monoclonal ED1 antibody, 1:500, Abcam, Cambridge, MA), and (4) perineurial fibroblasts (anti-glucose transporter-1 protein (anti-GLUT-1), mouse monoclonal, 1:500, Thermo-Fisher Sci., Life Technologies, Carlsbad, CA). GLUT-1 is highly expressed in perineurial fibroblasts and capillary endothelial cells when there is an intact nerve-blood barrier, but expression is significantly reduced after injury.[21] Secondary antibodies were goat anti-mouse Alexa 488 and goat anti-rabbit Alexa 594 (1:1000, Life Technologies, Carlsbad, CA). Blood vessel endothelial cells were labeled by incubation with a Tetramethyl rhodamine thiocyanate (TRITC) labeled lectin, *Bandeiraea simplicifolia*, (1:1,000, Sigma–Aldrich L-5264), which binds to blood vessel but not lymphatic endothelial cells.[22] Nuclei were labelled with 4′,6-diamidino-2-phenylindole (DAPI, 1:1000 in secondary antibody, Sigma-Aldrich). If not otherwise noted, supplies were from Thermo-Fisher.

Photography and image analysis

Using an upright Zeiss Axioplan Imaging 2e fluorescence microscope, color bright field images were taken with a Zeiss Axiocam digital camera and fluorescence images were taken in black and white, in each of three channels, with a QICam cooled CCS camera (Q Imaging, Canada) and combined into composites and pseudo colored using Photoshop (Adobe Systems Inc.) Analyses were done with Photoshop, NIH ImageJ and/or visual counts. Enhancement of staining via Photoshop was done to illustrate features in non-CT

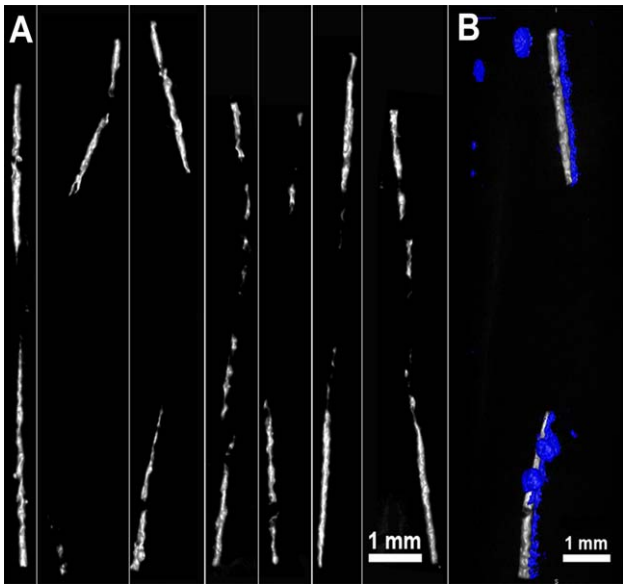

FIGURE 1. Micro-CT imaging of the Mg remaining in regenerating tissues within conduits at 6 weeks after repairing a short gap. (A) Mg filaments from all seven rats/conduits are shown, separated by spaces. The bar in the last panel applies to all other panels in A. (B) Low density material (blue) indicated the presence of gas bubbles adjacent to the wire in one animal.

images for figures, but was not used prior to any quantitative analysis.

Statistics

Quantitative data were collected by observers blinded to conditions. For normally distributed data, analyses were *t* tests or a one-way ANOVA with the Holm-Sidak post-hoc method and for non-normal data analyses were the Wilcoxon Rank Sum test or Kruskall–Wallis ANOVA on ranks with Dunn's post-hoc tests. For repeated measures, a repeated measure ANOVA and the Holm–Sidak post-hoc test were used. Analyses were performed with Matlab or Sigma Plot (v13) software. Significance was assigned with a p values of <0.05 and error bars show one standard deviation. Number of animals per group differed between assays due to technical issues or use in other assays, but no group had fewer than four animals. In the long-gap Mg group, two animals had no regenerating tissue within the conduit as determined by micro-CT imaging and histology and these animals were omitted from analyses ($n = 5$ for Mg).

RESULTS

Short gap repair: Magnesium resorption

The speed of Mg metal degradation *in vivo* depends on exposure to physiological salt solutions, which varies with site of implantation.[23] To evaluate metal degradation, regenerated tissues (plus conduits) were imaged by micro-CT at 6 weeks, after sacrifice of the short gap animals. As shown in Figure 1(A), there were significant gaps in all filaments, with the ends remaining more intact than central regions. Bubbles (low-density areas) were detected adjacent to the wire in one animal [Fig. 1(B)]. Bubbles indicate rapid Mg degradation, but this animal did not differ from others in the same group in any assay.

Short gap repair: Functional assessment

Functional measures showed no functional return in any group by 6 weeks post-surgery with the short gap. Atrophy of the calf muscle in live animals occurred rapidly after surgery, becoming significantly different from initial at 20 days post-surgery (DPS), with no differences between groups [Fig. 2(A), repeated measures two-way ANOVA (RM-2xANOVA), $p < 0.001$ for DPS, $p = 0.89$ for group and no interactions, $n = 7$ per group]. The weights of dissected calf muscles did not differ between groups [Fig. 2(B)] (ANOVA, $p = 0.94$). Values for pinch tests and foot extension dropped to 0 (no detection) and did not change by 6 weeks (data not shown).

Short gap repair: Histological assessment

Because the Ti filaments could not be sectioned, nor could the metal be removed without losing histological integrity, immunostaining was done using sections of nerve stumps distal to the filaments. Almost all animals displayed fascicles that were GLUT1+ and contained NF+ axons [Fig. 3(A–C, I–K)]. The total area inside GLUT-1+ fascicles (Fascicle Area) did not differ between groups [Fig. 3(D), ANOVA, $p = 0.87$, $n = 7, 5, 5$ for Em, Ti, Mg, for all short gap distal stump analyses]. The number of fascicles varied from 1 to 7, but averages per group were not different [Fig. 3(I–K) and graph 1E, ANOVA, $p = 0.12$ (averages not shown)]. Ti animals had only 3 or 4 fascicles/nerve (so only two points appear on the point plot) and nerves with fewer than three fascicles were only found in the Mg group. The percent area covered by NF+ staining within the fascicles (% area NF+) was significantly higher in the Mg group compared to Em or Ti [Fig. 3(F), ANOVA, $p = 0.003$]. The density of axons [Fig. 3(G), axonal density] did not differ between groups (ANOVA, $p = 0.27$), but the average size of stained axons (calculated from % area and density) was significantly different (ANOVA, $p = 0.04$), with Mg higher than Ti, but no other differences between groups (Mg = Em, Em = Ti). Thus, the presence of Mg had a significant effect on total amount of axonal material, and this was due primarily to differences in axonal size, not density.

Long gap repair: Functional assessment

At a longer time-period of survival (as with the longer gap size), there is a greater possibility of function returning. In terms of sensation, no animals responded to a skin pinch in the territories tested between surgery and 48 DPS [Fig. 4(A)]. Between 48 DPS and sacrifice, animals in all groups showed variable sensitivity to pinches at the ankle and postero-lateral side of the foot. However, only Iso animals developed sensitivity on the antero-lateral foot and lateral toe, and only after 60 DPS. This was consistently significant for the Iso group after 80 DPS (RM-2xANOVA, $p < 0.001$ for interactions, $n = 7,5,8$, for Em, Mg, and Iso groups). In terms of motor function, reflex extension of the lateral toe [Fig. 4(B)] dropped to zero after surgery for all animals and changes were seen only in the Iso group beginning at 69

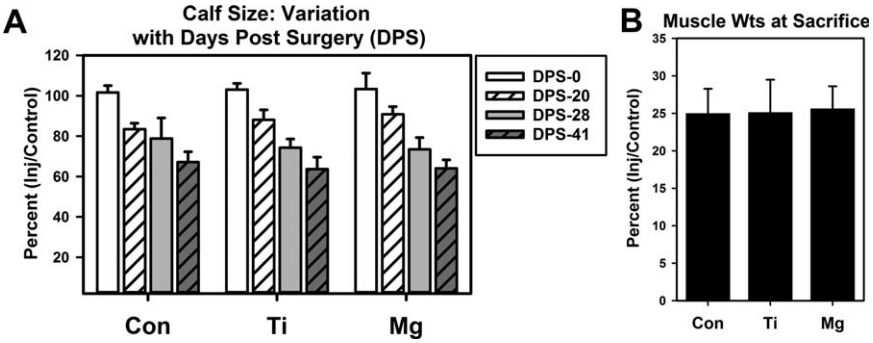

FIGURE 2. Functional assessment with a short gap, 6-week survival. (A) Live animal calf size measurements taken at designated days post-surgery (DPS), were expressed as injured calf size as a percent of contralateral, uninjured calf size in the same animal. (B) Wet weight of calf muscle at sacrifice.

DPS (RM-2xANOVA, $p < 0.001$ for interactions). The third measure, live animal calf size, decreased steadily after surgery, becoming significantly different from initial by 27 DPS in all groups and then plateauing at 60–70% of normal for Em and Mg groups [Fig. 4(C)] (RM-2xANOVA, $p < 0.001$ for groups, DPS and interactions). Variable differences occurred between 48 and 69 DPS, including Mg lower than both groups at 48 DPS; Iso higher than both at 63 DPS and Mg lower than Iso at 69 DPS, but these were neither consistent nor maintained. After 69 DPS, the Iso group was significantly higher than both other groups and Em = Mg, for all days measured. At sacrifice, the dissected calf muscles showed a reversal of atrophy only in the Iso group [Fig. 4(D), ANOVA, $p < 0.001$]. Thus, only the Iso group showed consistent and significant improvement for each live animal measure.

Long gap repair: Mg resorption

Mg resorption was not analyzed by micro-CT at sacrifice because it was anticipated that little or no Mg would remain and this was supported by both histology and other micro-CT analyses.

Long gap repair: Analysis by micro-CT

After fixation, the distal halves of the conduits plus nerves were osmium treated, embedded in resin and imaged via micro-CT, which allowed visualization of the soft tissues (Fig. 5). A 3 D reconstruction is shown in Figure 5(B) (tip

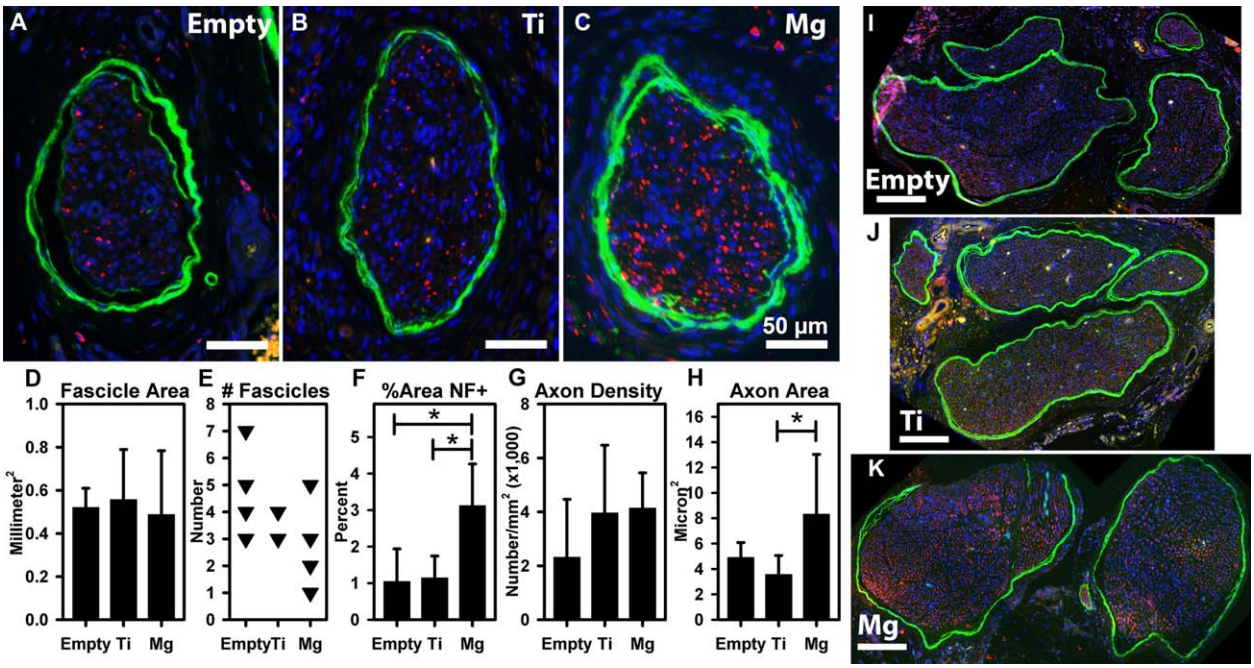

FIGURE 3. Short gap: Immunostaining of distal stumps of nerves after repair with either (A) an empty PCL conduit, (B) a conduit with a Ti filament or (C) a Mg filament. Axons are small dots (red in color images, anti-NF staining) within the brightly labeled circles (green in color images, anti-GLUT1 staining for the perineurium and endothelia of some small blood vessels). Bars = 50 µm. The graphs (D–G) show analysis of (D) total nerve area within GLUT1 stained fascicles, (E) number of fascicles per total nerve area per animal, (F) total percent area covered by NF staining within the fascicles, (G) average axon density in fascicles (number of NF+ fibers per mm^2), and (H) average axon size (micron2). Bars with asterisks show pairs significantly different. Immunostained images at lower magnification (I–K) (bars = 200 µm) show the variably sized fascicles.

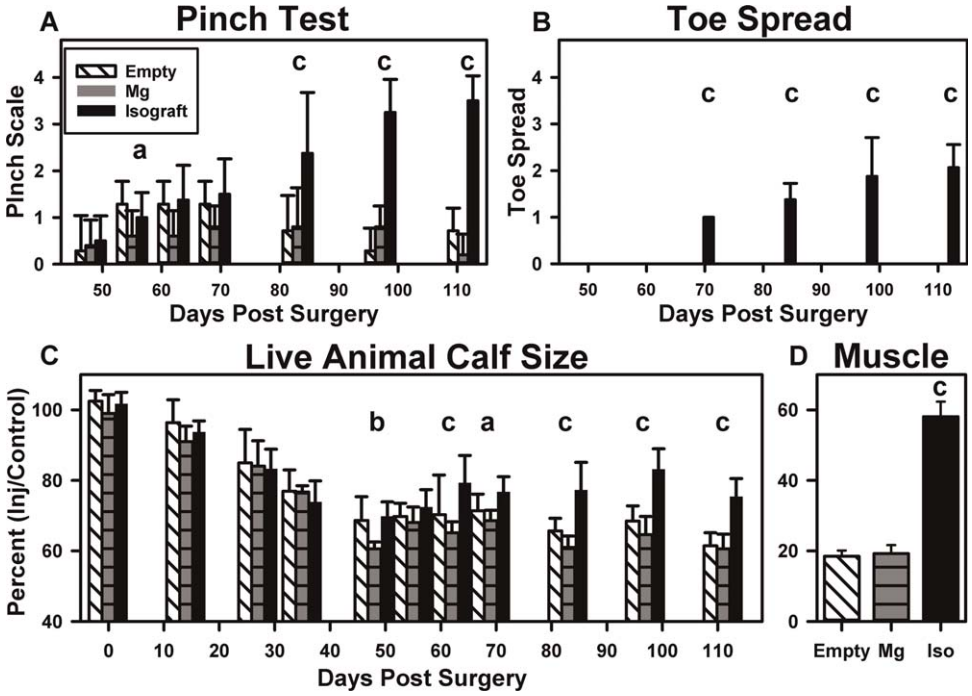

FIGURE 4. Functional assessment in the long gap experiment. Preset scales tested return of (A) sensation using a pinch test and (B) function using movement of the lateral toe on the injured foot. (C) Calf size was measured in living animals. (D) After sacrifice, the wet weight of dissected calf muscles was recorded. In C and D, injured leg measurements are given as a percent of uninjured leg measurements, per rat and averages per group are shown. The legend in A applies to all. Significance is indicated per DPS or measure, by small letters: (a) Mg different from Iso for that DPS, (b) Mg different from both other groups, (c) Iso group different from both other groups.

of white arrow is on conduit). Surrounding fat and muscle both appeared whiter (denser) than conduits or tissues. Using either the Inveon or ImageJ software, tissues could be viewed in three planes of section [Fig. 5(C–E,I)]. Osmium contrast allowed clear differentiation between conduits (black double-headed arrows in 5 C and D span the conduit), connective tissue external to the conduits and regenerating tissues inside the conduit. The density of the regenerating tissues (including both connective tissue and axons) was uniform and could be identified in the distal stumps because of differences with the surrounding, more fatty, tissues [black single headed arrows in Fig. 5(D)]. By selecting tissues with a specific density range in HU values, regenerating tissues in the distal stump could be identified (Fig. 5, blue in G), cropped and rendered in 3 D [Fig. 5(H)]. This allowed visualization of the multiple strands of regenerating tissues coursing through this area [Fig. 5(D,H)], presumably connecting with distal nerve tissue. The area of the internal tissues was measured inside the conduits [Fig. 5(F) shows an example of the tissue circled for measurement] and did not differ significantly between Em and Mg groups [Fig. 5(J), t-test]. No evidence of Mg metal was seen. The micro-CT images showed that two of the six animals in the Mg group lacked tissues at some point between the proximal midpoint and distal nerve stumps [very low density, Fig. 5(I), as seen in both sagittal and axial (insert) views]. The absence of tissues was confirmed by histological analysis (not shown). These two animals were omitted from all analyses, to determine effects only due to Mg presence (although analyses with and without showed no differences, data not shown). Also apparent was that the PCL conduit had developed cracks (probably due to PCL biodegradation and tissue pressures). Occasionally these cracks resulted in extension of the conduit into the lumen, giving an appearance of three walls [Fig. 5(I), black asterisks are on conduit pieces in both sagittal and axial (insert) views].

Long gap repair: Histological assessment of proximal nerve sections

Proximal halves of the conduits were paraffin embedded without osmication and sections were examined at three levels (proximal-1 = P-1, proximal-2 = P-2, and at the midpoint = Mid), as diagrammed in Figure 6(A). Because enlarged vessels were seen in H&E stained sections (not shown), staining was done with a lectin that binds to endothelial but not lymphatic lining cells, confirming that the majority were blood vessels [Fig. 6(F–I)]. Quantification of the average internal area per blood vessel (3+ images per nerve, averages per rat per group, termed BV size) is shown in Figure 6(B) and of the total area inside blood vessels (as % of area imaged, averaged per rat and group, termed Area Covered) is shown in Figure 6(C), for two levels of sections. At the P-1 level, there were no differences between groups in either measure (ANOVA, BV size $p > 0.24$, Area $p = 0.86$, $n = 5,4,4$, Em, Mg, Iso). However, deeper in the conduits (P-2 and Mid level data were combined after determining a lack of difference via ANOVA), significant differences were

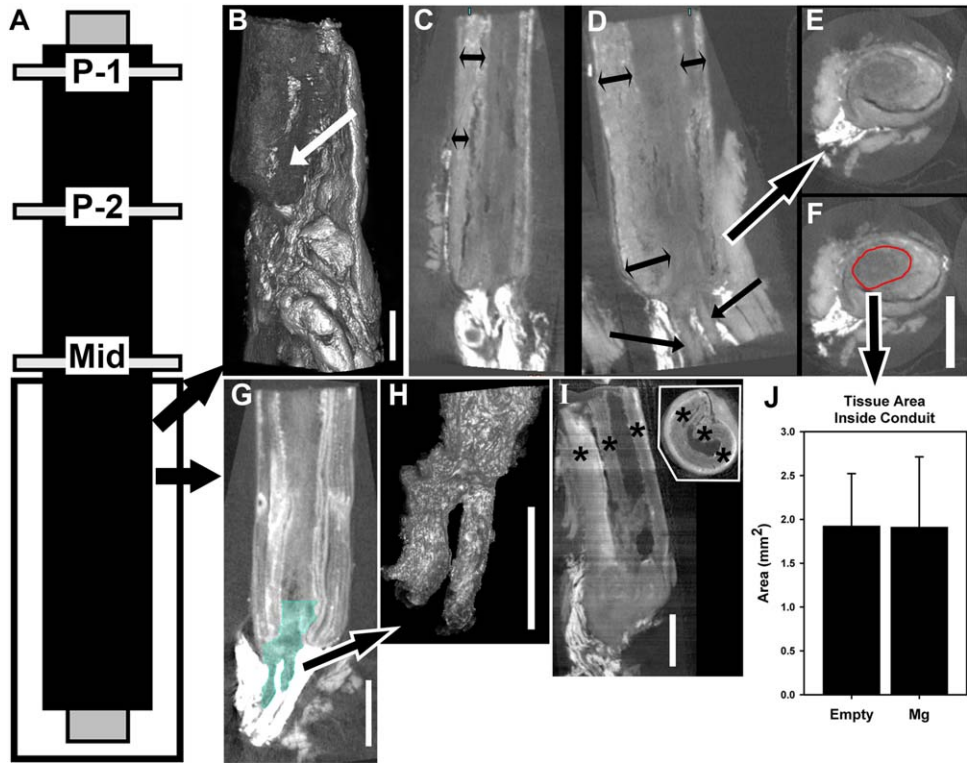

FIGURE 5. Micro-CT imaging of osmicated regenerating tissues in distal conduit halves. (A) Diagram of tissue processing scheme. Distal halves were osmicated and imaged. (B) 3 D rendering for one animal (arrow tip is on conduit material). (C–F) Images of one conduit in three planes [two sagittal (C,D), one axial (E,F)]. Double black arrows span conduit. Single headed black arrows show tissue strands at the distal end that appear to interconnect internal tissues to distal nerve material. Black + white single headed arrow shows approximate level of the axial slice in E and F. (F) The area of regenerating tissues was measured (red circle, F) to give the graph in J. (G) Using the Inveon Software, areas of regenerating tissues with the same HU values were selected (blue in G), cut out and rendered in 3 D (H). In (I), for one Mg group rat, the low tissue density inside the conduit indicated a lack of tissues and incomplete regeneration. Black asterisks in (I) are on conduit material in the sagittal view and in the axial view (insert). (J) Graph of average area of tissues within the conduits, measured with ImageJ. Bars are 2 mm in all, and the bar in F applies to C–F.

seen in both BV size [Fig. 6(D)] and Area Covered [Fig. 6(E)]. For BV size, both Em and Mg groups were greater than Iso, with Em = Mg (ANOVA, $p = 0.002$, $n = 6,4,5$, Em,Mg,Iso). For Area Covered, Em was greater than both other groups and Mg = Iso (ANOVA $p < 0.001$). The lectin staining at P-2 or Mid levels is shown in Figure 6(F–I).

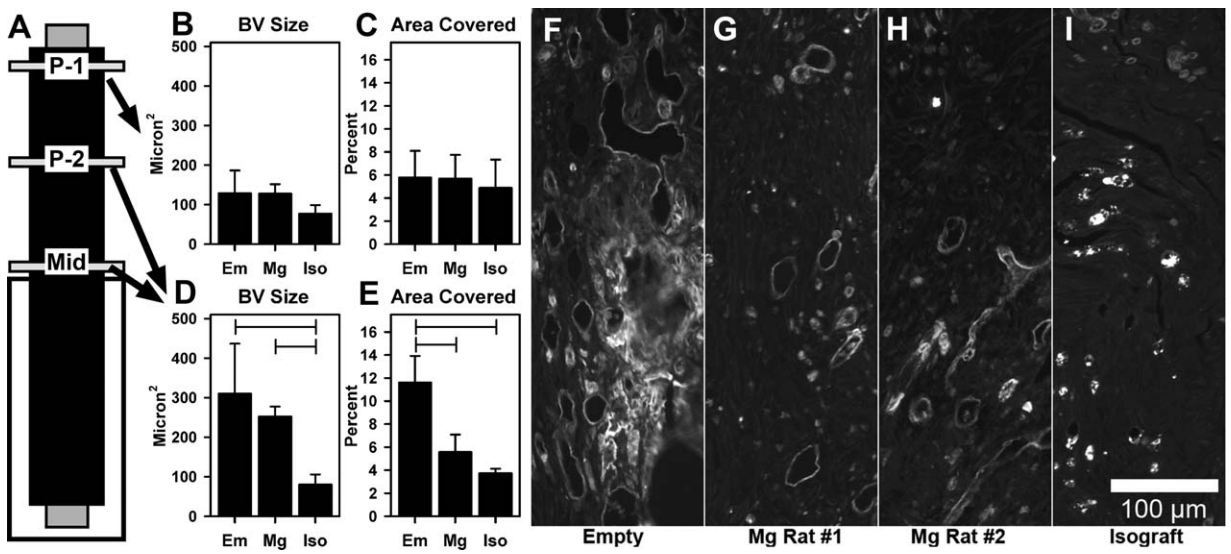

FIGURE 6. Histological analyses of proximal tissues. (A) Diagram shows the three levels (P-1, P-2, Mid) chosen for histological examination. (B–E) Graphs of analysis of lectin staining: (B, C) BV size and Area Covered in sections at the P-1 level. (D, E) BV size and Area Covered in combined data from P-2 and Mid sections. (F–I) Fluorescent lectin staining in 4 rats (empty, two Mg and one Allograft). Bar in I applies to F–I.

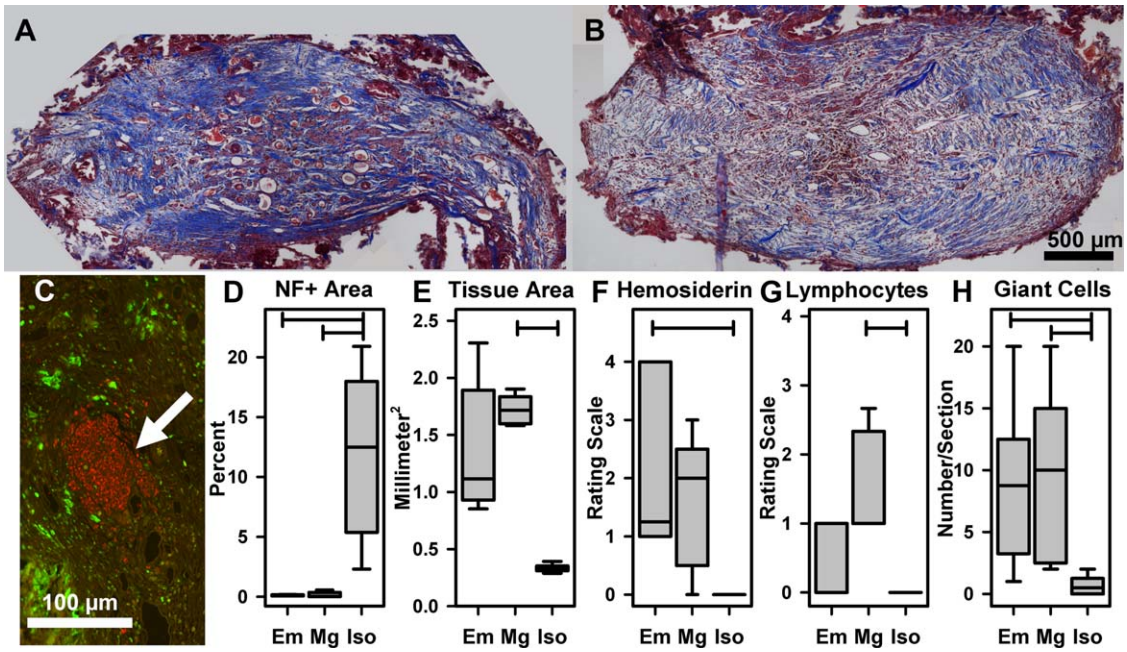

FIGURE 7. (A, B) Masson's trichrome stain in Empty (A) and Mg (B) sections. The conduit material (mostly out of view or missing) appears as red, irregularly shaped remnants rimming the tissue. (C) Immunostaining (at C level) for NF (red) and ED1 (green). Arrow points to a cluster of NF+ axons centrally located in the conduit. Bar = 100 μm. (D) Percent area covered by NF staining in C level sections. (E) Total area of regenerating tissue in C level sections. (F) Scored for amount of hemosiderin staining (virtually none in Iso group). (G) Scored for the amount of lymphocyte infiltration. (H) Counts of giant cells in the nerve area. Bars show pairs with significant differences.

Thus, the Em group had greater expansion of blood vessels within the conduits.

Masson's trichrome stain was used to examine collagen deposition, a measure of fibrosis (Fig. 7(A,B), collagen is deep blue]. While variability prevented quantification, there were no obvious qualitative differences in the amounts of condensed collagen between Em (7 A) and Mg (7B) groups. Also, no fibrotic scarring was seen that could be attributed to a reaction to the degraded Mg metal.

Axonal extension to the midpoint was analyzed by quantifying NF+ staining in Mid level sections [Fig. 7(C) shows a cluster of axons at tip of arrow, Em group animal]. The percentage of NF+ [Fig. 7(D)] was lower for both Em and Mg groups than Iso and Em = Mg (ANOVA on ranks, $p = 0.005$, $n = 5,5,6$, Em,Mg,Iso, Dunn's post-hoc test).

The total area of regenerating tissue in Mid level sections [Fig. 7(E), tissue area in mm^2] showed that the Mg group was larger than the Iso group (post-hoc significance $p = 0.003$) and the Em difference trended higher (post-hoc $p = 0.072$), with Em = Mg (ANOVA on ranks, $p = 0.003$, Dunn's post-hoc). The histology was more variable than the micro-CT analyses.

Using H&E stained sections (not shown), inflammatory markers were scored by two observers blinded to condition. Scales of 0–4 (4 = abundance) were used to rate the presence of hemosiderin [pigment usually found within phagocytes, remaining from disruption of red blood cells that extravasate following either angiogenesis or inflammation, Fig. 7(F)] and extravascular lymphocytes [increases with increased inflammatory status, Fig. 7(G)]. For hemosiderin, Em was higher than Iso (post-hoc $p = 0.014$), with a trend toward Mg higher than Iso (post-hoc $p = 0.061$) and Em = Mg (ANOVA on ranks, $p = 0.007$). For lymphocytes, Mg was higher than Iso (*post hoc* $p = 0.011$) and Mg = Em (ANOVA, $p = 0.109$) and Em = Iso (ANOVA $p = 0.003$). Numbers of foreign body giant cells [multi-nucleated cells that form in reaction to foreign biomaterials, Fig. 7(H), per tissue area, per section] were significantly higher for Mg and Em vs. Iso (*post hoc* $p = 0.025$ and 0.026) and Mg = Em (ANOVA on ranks, $p = 0.008$).

DISCUSSION

The results suggest that, with a short gap and at 6 weeks post-repair, the presence of a Mg metal filament was beneficial for axon nerve regeneration. Increases were seen in total amount of axonal material and this was in large part due to increased size of the axons (Mg was different from Ti). While further analysis of myelin parameters would be needed to confirm an increase in axon volume, an increased size of axons is promising because diameter determines conduction velocity and is a good determinant of eventual functional recovery.[24] The fact that Mg was different from Ti metal filaments suggests that the beneficial effects of Mg are not due to simple physical support. Advantages could include that Mg is not as stiff as Ti,[25] leading to less tissue irritation, the Mg ions released by Mg degradation have neuroprotective or anti-inflammatory effects,[15,26] or the highly conductive nature of Mg metal (higher than Ti, unpublished results) results in short-term electrical stimulation of nerve regeneration, which is known to enhance nerve regeneration.[27] However, functional improvement was not seen for the short gap, at 6 weeks. While 6 weeks is usually

considered too early to expect changes, some groups have demonstrated differences at that time.[20]

In the longer gap experiment and 16 weeks post-repair, significant functional improvement was seen only with the Iso group. Two animals in the Mg group showed a lack of tissue at the midpoint, suggesting a lack of regeneration, but the removal of these animals from behavioral analyses did not affect the functional outcomes (data not shown). Thus, the short gap benefits were not observed with a longer gap and longer time-period.

Some of our "functional" measures and findings were unusual compared to other studies. Measuring calf size in living rats, which was done using a thread held around the leg at the midpoint of the muscle, is not a usual measure and includes several sources of variability. The sources of variability included (a) the person analyzing (this measure was best done by one person throughout), (b) the degree of muscle contraction (how much the rat was pulling against having its leg held), (c) differences in subcutaneous fat or thickness of skin (which could vary with hydration status), and (d) thickness of hair. The differences in fat, skin and hair were minimized by using the metric of injured leg as a percent of uninjured and the degree of muscle contraction was minimized by waiting until the rat was relatively relaxed. Despite the variability, we were able to distinguish steady atrophy in all groups and significant muscle size improvement only in the Iso group and after 80 DPS. The pattern (improvement in just the Iso group) was consistent with all other measures. The goal of measuring calf size was to determine effects of experimental treatments on atrophy rate. The Mg animals did show a significant decrease in calf size at ~6 weeks, which is when Mg was presumably in the process of resorbing, as per micro-CT imaging in the short-term experiment. However, the difference between groups was not pronounced nor continued, so further work was not judged to be warranted at this point, for example, by analyzing earlier time points with the longer gap length.

The pinch response measure along the lateral foot showed a return of sensitivity to a skin pinch at the ankle and back of the foot beginning around 45 DPS, while sensitivity on the antero-lateral foot and lateral toe was only observed in the Iso group and after 60 DPS. We attribute the sensory returns in the posterior areas (and the variable returns to toes 3–4, not shown) to expansion of the territory of the saphenous nerve. Expansion of territory has been described previously, detectable as early as 5 weeks.[28] Von Frey hairs were not used because pinching with forceps with a small tip area allowed better spatial control. False positives could have occurred if von Frey hair use was not carefully restricted to near or on the lateral toe. Other observations with the pinch test included that it was necessary to (a) pinch only a small patch of skin or between toe joints, (b) avoid moving the toe or adjacent areas of skin, and (c) keep the animal from seeing what was being done. Any toe, joint or sizable skin movement, or anticipation of a pinch, could trigger a false reaction. Pinch strength was increased to levels similar to those triggering a response in control areas, but the force was not controlled nor measured. Electronic measurement of pinch strength might have added additional information, but the forceps tips would have to be small enough to allow accurate placement.

For toe spread, only animals in the Iso, long-gap group showed any return of movement of the lateral toe. Improvement in just the Iso group was consistent with all other measures. Toe movement was possible to score even with a foot contracture (assigned a value of 1–3 depending on extent of movement). The ability to analyze contracted feet is an advantage over the standard sciatic functional index (SFI) or static sciatic index (SSI) scores, which cannot be calculated when contractures result in the rats walking or standing on the side or dorsum of the foot. Toe movement also showed consistent progression over time in the Iso group and the pattern was consistent with sensory values, so we feel that this measure was valid for evaluating nerve repair.

In the long-term Mg group, when intact tissue was present, there were signs of improved tissue health. The most significant improvement in the Mg group compared to Em was the reduction in area taken up by blood vessel lumens. A reduction in lumen area was presumed to be improvement because an even smaller area was covered by lumens in the Iso group (and in normal nerves, data not shown). Furthermore, the vessels in the Em and (to a lesser degree) in the Mg group appeared abnormal, with irregular lumens and unusually thin walls for lumen size, and were more like lymphatic vessels than blood vessels. However, the lectin staining showed that they were blood vessels. Blood vessel enlargement is known to be an indication of inflammation.[29] Because an improvement in blood vessel characteristics in the Mg vs. Em group was detected after full Mg degradation, this suggests that Mg presence made long-term changes in tissues. Some tissue health improvement in the Mg group was also suggested by the lower hemosiderin load, but this was perhaps offset by the increased lymphocyte load. In terms of fibrosis, which occurs in the foreign body response,[30] there were no consistent differences between Mg and Em groups, suggesting a similar degree of tissue reaction. No signs of necrosis or tissue disruption were observed in the Mg group, which fits with a similar lack of necrosis in our previous findings.[17] It is also consistent with the idea that the degradation of the Mg was gradual, because the amount of Mg might have been toxic if resorption had occurred immediately after placement (a total of ~1,986 mM Mg, given the estimated area of the conduit cavity). Other implant studies have shown a similar lack of Mg metal toxicity around implants.[25]

Another observation was that the Iso group had significantly smaller total tissue size than either conduit group. In sections stained with trichrome (Fig. 7) and H&E (not shown), the Mg and Em groups had not only larger and more blood vessels, but also more edema and fibrosis, all of which occur during normal tissue repair, as in wound repair. The regenerating tissues also expanded to fill almost all the conduit space by 16 weeks, so their total size was constrained only by the conduit. With isografts, the original

connective tissues of the donor nerve remain intact after grafting. Because these connective tissues are not significantly expandable, they presumably constrained tissue growth, including edema and fibrosis. It is therefore interesting that a greater percentage of axons was seen per nerve area in the Iso group, despite the smaller (and denser) tissue area available for axons to penetrate through. Overall, our data support the idea that the presence of Mg does not block the small amount of nerve regeneration that can occur in conduits without added growth factors or cells, and Mg may also have other beneficial effects on regenerating tissues.

Of note was that the 15-mm gap was not a critical gap for the long-term experiment with these particular PCL conduits; all Em group animals had tissue regrowth. However, a 1.5-mm gap size in adult rats is maximal and may have caused compression of the Mg filaments. Compression stress could have affected Mg degradation rate or caused metal breakage that might have interfered with regeneration. Thus, another animal model might be needed to more thoroughly test the hypothesis that Mg metal filaments overcome the problem of a critical gap size.

Mg degradation in the short gap experiment was more extensive at 6 weeks than we observed previously with the same time, gap length, conduits and saline filler, where regeneration appeared to be enhanced when filaments remained intact.[17] The more extensive resorption in the current experiment might be explained by the use of a straightening technique, which was necessary to place filaments in longer conduits. Although the straightening procedure was mild, it may have accelerated corrosion due to cracking or pitting. As we observed previously.[17] degradation was more extensive in the middle of the filaments. We speculate that the rapid ingrowth of cells from both nerve stumps provides greater protection of the filaments at the ends by reducing exposure to liquid and protecting Mg from bending stresses, both of which accelerate Mg degradation. If a slower degradation rate is needed, which may be true for longer gaps than were tested here, then methods that slow Mg degradation need to be explored. Mg degradation can be slowed by alloying with other metals, altering the surface (anodization or physical treatment) or coating with water-resistance substances like polymers.[11]

As in our previous experiments, Mg filaments were biocompatible with nerve repair. We show here that Mg filaments can improve regeneration across a short nerve gap, but not a longer gap. One explanation for less regrowth over a longer gap could be that, while Mg ions are neuroprotective after nervous tissue damage (brain injury) in animals,[15] they may not actually stimulate extensive nerve outgrowth. We saw very little stimulation of neurite outgrowth in cell culture experiments with differentiated neural stem cells, after raising exogenous Mg.[31] Therefore, the full benefits of using Mg filaments in peripheral nerve repair may not be seen unless combined with use of an additional axonal outgrowth-stimulating factor.

Micro-CT imaging of soft tissues was possible after using osmium as a contrast agent. The use of osmium to enhance soft tissue contrast in micro-CT imaging has been demonstrated previously.[32] Imaging allowed a relatively rapid identification that two conduits had no internal tissues. It was also very useful for understanding the relationship between conduit materials and regenerating tissues and for understanding how the conduit was degrading and being affected by tissue pressures. However, osmium infiltration with resin embedding had several disadvantages. Most significant was that tissue penetration was variably incomplete, with poor staining of some central areas within conduits and muscles (not shown). This confirms literature data where osmication is said to penetrate only $\sim$1 mm thick.[32] Our tissues were $\sim$ 2 mm in diameter. We have seen much better penetration and more successful micro-CT imaging with iodine as a contrast agent.[33]

CONCLUSIONS

Mg filaments placed within a nerve guide were well tolerated and biocompatible with tissue regrowth within nerve conduits, including axon regeneration. Their presence improved axonal growth over a short nerve injury gap, after a relatively short time-period *in vivo*, compared to conduits alone or with a Ti filament. With a longer gap and longer time-period, neither functional improvement nor increased axonal growth was observed compared to empty conduits. However, the presence of the Mg filament had some beneficial effects on tissue inflammation. Thus, the use of Mg filaments inside nerve conduits has potential for use in nerve regeneration, although further refinement is needed to optimize the potential.

ACKNOWLEDGMENTS

The authors thank Kathleen LaSance, Director of the Vontz Core Imaging Laboratory, for providing micro-CT imaging and guidance on CT image manipulation, and Ami Cohen, Erin Armao and James Liggett for technical assistance. Any opinions, findings, and conclusions or recommendations expressed in this material are those of the authors and do not necessarily reflect the views of any of the funding agencies.

REFERENCES

1. Deumens R, Bozkurt A, Meek MF, Marcus MAE, Joosten EAJ, Weis J, Brook GA. Repairing injured peripheral nerves: Bridging the gap. Prog Neurobiol 2010;92:245–276.
2. Rinker B, Vyas KS. Clinical applications of autografts, conduits, and allografts in repair of nerve defects in the hand: Current guidelines. Clin Plast Surg 2014;41:533–550.
3. Daly W, Yao L, Zeugolis D, Windebank A, Pandit A. A biomaterials approach to peripheral nerve regeneration: Bridging the peripheral nerve gap and enhancing functional recovery. J R Soc Interface 2012;9:202–221.
4. Carriel V, Alaminos M, Garzón I, Campos A, Cornelissen M. Tissue engineering of the peripheral nervous system. Expert Rev Neurother 2014;14:301–318.
5. Kehoe S, Zhang XF, Boyd D. FDA approved guidance conduits and wraps for peripheral nerve injury: A review of materials and efficacy. Injury 2012;43:553–572.
6. Yannas IV, Zhang M, Spilker MH. Standardized criterion to analyze and directly compare various materials and models for peripheral nerve regeneration. J Biomater Sci Polym Ed 2007;18:943–966.

7. Zhang M, Yannas IV. Peripheral nerve regeneration. Adv Biochem Eng/Biotech 2005;94:67–89.
8. Clements IP, Kim Y, English AW, Lu X, Chung A, Bellamkonda RV. Thin-film enhanced nerve guidance channels for peripheral nerve repair. Biomaterials 2009;30:3834–3846.
9. Huang W, Begum R, Barber T, Ibba V, Tee NCH, Hussain M, Arastoo M, Yang Q, Robson LG, Lesage S, Gheysens T, Skaer NJV, Knight DP, Priestley JV. Regenerative potential of silk conduits in repair of peripheral nerve injury in adult rats. Biomaterials 2012;33:59–71.
10. Whitlock EL, Tuffaha SH, Luciano JP, Yan Y, Hunter DA, Magill CK, Moore AM, Tong AY, Mackinnon SE, Borschel GH. Processed allografts and type I collagen conduits for repair of peripheral nerve gaps. Muscle Nerve 2009;39:787–799.
11. Walker J, Shadanbaz S, Woodfield TBF, Staiger MP, Dias GJ. Magnesium biomaterials for orthopedic application: A review from a biological perspective. J Biomed Mater Res B Appl Biomater 2014;102:1316–1331.
12. Luthringer BJC, Feyerabend F, Römer RW. Magnesium-based implants: A mini-review. Magn Res 2014;27:142–154.
13. Windhagen H, Radtke K, Weizbauer A, Diekmann J, Noll Y, Kreimeyer U, Schavan R, Stukenborg-Colsman C, Waizy H. Biodegradable magnesium-based screw clinically equivalent to titanium screw in hallux valgus surgery: Short term results of the first prospective, randomized, controlled clinical pilot study. Biomed Eng Online 2013;12:1–10.
14. Zheng YF, Gu XN, Witte F. Biodegradable metals. Mater Sci Eng R Rep 2014;77:1–34.
15. Sen AP, Gulati A. Use of magnesium in traumatic brain injury. Neurotherapeutics 2010;7:91–99.
16. Takeuchi S, Nagatani K, Otani N, Nawashiro H, Sugawara T, Wada K, Mori K. Hydrogen improves neurological function through attenuation of blood-brain barrier disruption in spontaneously hypertensive stroke-prone rats. BMC Neurosci 2015;16.
17. Vennemeyer JJ, Hopkins T, Hershcovitch M, Little KD, Hagen MC, Minteer D, Hom DB, Marra K, Pixley SK. Initial observations on using magnesium metal in peripheral nerve repair. J Biomater Appl 2015;29:1145–1154.
18. Kokai LE, Lin Y, Oyster NM, Marra KG. Diffusion of soluble factors through degradable polymer nerve guides: Controlling manufacturing parameters. Acta Biomater 2009;5:2540–2550.
19. Kokai LE, Bourbeau D, Weber D, McAtee J, Marra KG. Sustained growth factor delivery promotes axonal regeneration in long gap peripheral nerve repair. Tissue Eng Part A 2011;17:1263–1275.
20. Siemionow M, Duggan W, Brzezicki G, Klimczak A, Grykien C, Gatherwright J, Nair D. Peripheral nerve defect repair with epineural tubes supported with bone marrow stromal cells. A Preliminary Report. Ann Plast Surg 2011;67:73–84.
21. Stark B, Carlstedt T, Cullheim S, Risling M. Developmental and lesion-induced changes in the distribution of the glucose transporter Glut-1 in the central and peripheral nervous system. Exp Brain Res 2000;131:74–84.
22. Baluk P, McDonald DM. Markers for Microscopic Imaging of Lymphangiogenesis and Angiogenesis. Ann N Y Acad Sci 2008;1131:1–12.
23. Witte F, Hort N, Vogt C, Cohen S, Kainer KU, Willumeit R, Feyerabend F. Degradable biomaterials based on magnesium corrosion. Curr Opin Solid State Mater Sci 2008;12:63–72.
24. Raimondo S, Fornaro M, Di Scipio F, Ronchi G, Giacobini-Robecchi MG, Geuna S. Chapter 5 methods and protocols in peripheral nerve regeneration experimental research. Part II—Morphological techniques. Int Rev Neurobiol 2009;87:81–103.
25. Durisin M. Bioabsorbable Behaviour of Magnesium Alloys—An In Vivo Approach. In: Anonymous Surface Modification of Magnesium and its Alloys for Biomedical Applications. New York, USA: Woodhead Publishing, Elsevier; 2015. p 123–178.
26. de Baaij JH, Hoenderop JG, Bindels RJM. Magnesium in man: Implications for health and disease. Physiol Rev 2015;95:1–46.
27. Gordon T. Electrical stimulation to enhance axon regeneration after peripheral nerve injuries in animal models and humans. Neurotherapeutics 2016;13:295–310.
28. Duraku LS, Hossaini M, Hoendervangers S, Falke LL, Kambiz S, Mudera VC, Holstege JC, Walbeehm ET, Ruigrok TJH. Spatiotemporal dynamics of re-innervation and hyperinnervation patterns by uninjured CGRP fibers in the rat foot sole epidermis after nerve injury. Mol Pain 2012;8:1–13.
29. Huggenberger R, Detmar M. The cutaneous vascular system in chronic skin inflammation. J Investig Dermatol Symp Proc 2011;15:24–32.
30. Anderson JM, Rodriguez A, Chang DT. Foreign body reaction to biomaterials. Semin Immunol 2008;20:86–100.
31. Vennemeyer JJ, Hopkins T, Kuhlmann J, Heineman WR, Pixley SK. Effects of elevated magnesium and substrate on neuronal numbers and neurite outgrowth of neural stem/progenitor cells in vitro. Neurosci Res 2014;84:72–78.
32. Metscher BD. MicroCT for developmental biology: A versatile tool for high-contrast 3D imaging at histological resolutions. Dev Dyn 2009;238:632–640.
33. Hopkins TM, Heilman AM, Liggett JA, LaSance K, Little KJ, Hom DB, Minteer DM, Marra KG, Pixley SK. Combining microcomputed tomography with histology to analyze biomedical implants for peripheral nerve repair. J Neurosci Methods 2015;255:122–130.